Disintegration of Li⁶ by Deuterons*
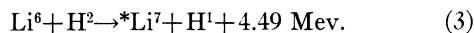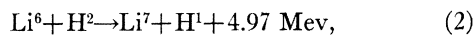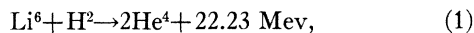
WARD WHALING** AND T. W. BONNER

The Rice Institute, Houston, Texas

(Received April 10, 1950)

The cross sections of the Li⁶$(d,\alpha)\alpha$ and Li⁶(d,p)Li⁷, *Li⁷ reactions have been measured up to energies of 1600 kev. Evidence of a resonance level in Be⁸ for 347 kev deuterons is presented. The angular distribution of the two proton groups has been observed at 400, 600, 1000, and 1400 kev. The complexity of the angular distribution increases with bombarding energy, requiring a P_6 term in the Legendre polynomial expansion at the highest bombarding energy.

I. INTRODUCTION

THE study of the nuclear reactions that take place when Li⁶ is bombarded by deuterons has been hampered in the past by the presence of the much more abundant Li⁷ isotope, which takes part in similar reactions under deuteron bombardment. When lithium enriched in the mass six isotope became available through the AEC, it was felt worth while to re-examine the Li⁶+H² reactions, and this paper reports observations on the following reactions.

$$\text{Li}^6 + \text{H}^2 \rightarrow 2\text{He}^4 + 22.23 \text{ Mev}, \tag{1}$$

$$\text{Li}^6 + \text{H}^2 \rightarrow \text{Li}^7 + \text{H}^1 + 4.97 \text{ Mev}, \tag{2}$$

$$\text{Li}^6 + \text{H}^2 \rightarrow {}^*\text{Li}^7 + \text{H}^1 + 4.49 \text{ Mev}. \tag{3}$$

The Q-values above are calculated from Bethe's 1947 values of the nuclear masses.[1] The lithium six targets were prepared from lithium sulfate enriched to 95
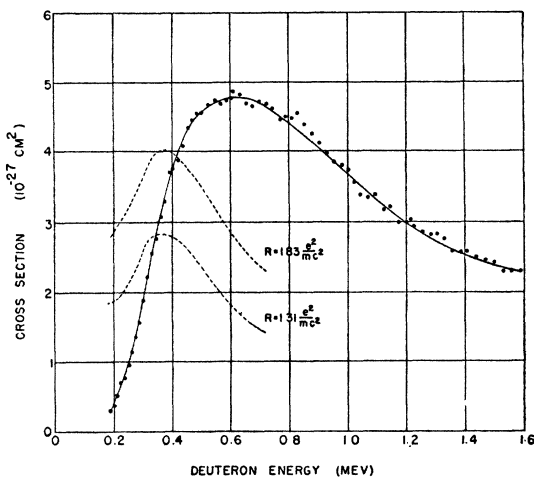

FIG. 1. Cross section for emission of alpha-particles into unit solid angle at 90°. The two dotted curves indicate the excitation function corrected for the penetrability of incident deuteron, assuming two different values of the radius of the Li⁶+H² system. The units for the dotted curves are arbitrary.

[1] H. A. Bethe, *Elementary Nuclear Theory* (John Wiley & Sons, Inc., New York, 1947).

percent Li⁶, obtained from the Isotopes Branch, Atomic Energy Commission, Oak Ridge, Tennessee.

II. ALPHA-PARTICLE EXCITATION FUNCTION

The cross section for the reaction Li⁶+H²→2He⁴ +22.23 Mev has been determined as a function of deuteron energy over the energy range from 190 kev to 1600 kev. The target, a thin layer of Li₂⁶SO₄ (150 micrograms per cm²), evaporated in vacuum on a thick silver disk, was set at an angle of 45° to the deuteron beam from the Rice Institute pressure Van de Graaff generator. Alpha-particles emitted at an angle of 90° to the beam were detected with a proportional counter, with a window subtending a solid angle of 1.72×10⁻³ steradian. Sufficient aluminum absorber was placed in front of the counter window to stop the shorter range alphas from the Li⁷(d,n)2He⁴ reaction; the long range protons from the Li⁶(d,p)Li⁷, *Li⁷ reactions were biased out with a discriminating circuit.

The experimental results are shown in the solid curve in Fig. 1. Each point on the curve represents a count of at least 2560 alphas, and the separation between adjacent points on the curve is approximately one-half the target thickness. The energy spread of the deuterons passing through the magnetic analyzer is 10 kev.

The cross section indicated in Fig. 1 is the number of alpha-particles emitted into unit solid angle at 90° per deuteron incident on a target of one Li⁶ nucleus per sq. cm, as calculated from the experimental geometry and the target thickness. The target thickness was determined by weighing the target disk before and after evaporation of the Li₂SO₄ upon it. This introduces an uncertainty of 20 percent in the quoted cross section, since it is not known whether the one water of hydration molecule normally present with each Li₂SO₄ molecule appears in a target prepared in this manner and exposed to the atmosphere for periods of from several minutes to several hours before weighing. The cross section has been calculated on the assumption that this water of hydration is not present.

The peak in the alpha-particle excitation curve near 600 kev lies in the energy region in which the increasing penetrability of the incident deuteron through the barrier at the Li⁶ nucleus will displace the peak in the experimental excitation curve above the resonant energy. An accurate correction for this penetrability

factor requires a better understanding of the effective radius of the $Li^6 + H^2$ system than is available at present. We have calculated the penetrability correction for two extreme values of the radius, with the expectation that the correct value of the resonant energy will lie somewhere between the two values obtained in this way.

The Gamow penetrability factor $P_l(E)$ for s-deuterons has been calculated after the method given by Bethe.[2] That s-deuterons excite this level in Be^8 seems likely from the angular distribution of the emitted alphas and the magnitude of the cross section.[3] For the larger value of the effective nuclear radius we have taken 1.83 e^2/mc^2, as suggested by Resnick and Inglis, which is equivalent to attributing to the deuteron an effective radius equal to that of the Li^6 nucleus determined from the $(e^2/2mc^2)A^{\frac{1}{3}}$ relation. For the smaller value we have taken $1.31e^2/mc^2$, somewhat smaller than the value 1.5 e^2/mc^2 proposed for the $Li^7 + H^1$ system.[4,5]

The function $\sigma(90°)/[P_0(E)\lambda^2]$ is plotted in the two dotted curves in Fig. 1 for the two different choices of the nuclear radius; λ is the wave-length of the incident deuteron; $P_0(E)$ is the penetrability factor for s-deuterons incident on the Li^6 nucleus; $\sigma(90°)$ is the cross section for alpha-particle emission into unit solid angle at 90°. These corrected curves show more clearly the behavior of the resonance denominator, with a peak at the resonant energy E_R. For $r = 1.31$ e^2/mc^2, $E_R = 380$ kev; and for $r = 1.83$ e^2/mc^2, $E_R = 374$ kev. The thickness of the target of 150 micrograms per sq. cm Li_2SO_4 is approximately 60 kev for 380 kev deuterons, calculated from the stopping power of the constituents of the target. Subtracting one-half the target thickness from the mean value of E_R, the resonant energy is 347 kev in the laboratory system, which corresponds to an excitation energy of 22.46 Mev in Be^8.

The use of $\sigma(90°)$ instead of the total cross section is justified by the slight deviation from spherical symmetry in the angular distribution of the alpha-particles at this low bombarding energy. In estimating the width of this level it becomes necessary to consider the shape of the excitation curve at higher energies, where the angular distribution becomes asymmetric, and the total cross section must be used. This total cross section was calculated using our value of $\sigma(90°)$ and the angular distribution data of Heydenburg et al. given in reference 3. After making the penetrability correction outlined above, the level width at half maximum appears to be of the order of 520 kev.

III. PROTON EXCITATION FUNCTION

The excitation curves for the two groups of protons from the reactions (2) and (3) have been determined over the energy range from 200 kev to 1800 kev. The $Li_2^6SO_4$ target was evaporated on a thin silver foil

[2] H. A. Bethe, Rev. Mod. Phys. **9**, 163 (1937).
[3] R. Resnick and D. R. Inglis, Phys. Rev. **76**, 1318 (1949).
[4] D. R. Inglis, Phys. Rev. **74**, 21 (1948).
[5] R. F. Christy and R. Latter, Rev. Mod. Phys. **20**, 185 (1948).

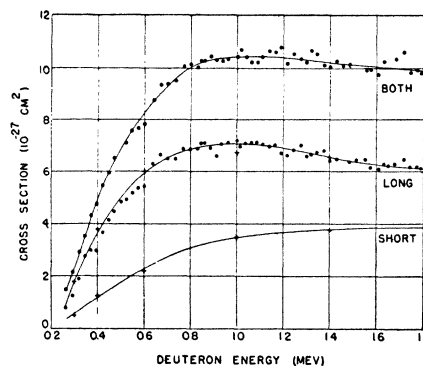FIG. 2. Cross section for emission of long and short range protons into unit solid angle at 0°.

which was just thick enough to stop the deuteron beam, and protons emitted in the direction of the beam were detected in a proportional counter after passing through the silver target backing. Several targets were used—a thicker one at low bombarding energy where the yield is low, and thinner ones at high energy to improve the resolution of the two groups of protons.

The two groups were separated by placing in the proton path aluminum absorbers, variable in steps of 3 mm air equivalent. At each bombarding energy the shape of the integral range-numbers curve was determined by observing the counting rate with different amounts of absorber in front of the counter window, and the counting rate for the two groups together and for the longer group alone estimated from the counting rate on the plateaus in the integral range-number curve. The difference in these two counting rates gives the counting rate for the short proton group; no charged particles of range greater than that of the protons in reaction (2) were observed.

The experimental results plotted in Fig. 2 have been corrected for the variation with bombarding energy of the solid angle subtended by the counter in center of mass angle (the solid angle subtended by the counter window at the target is 1.08×10^{-3} steradian). This correction has been calculated from the Q-value 4.97 Mev, and used for both groups of protons; the correction differs from that for $Q = 4.49$ Mev by only 3 percent at 1.0 Mev bombarding energy.

At low energies the curves for the individual groups have been drawn through the crossed points, which are
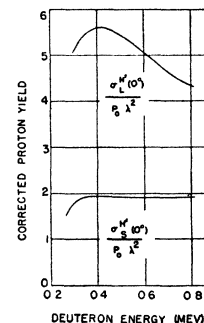

FIG. 3. Excitation curves for long and short range protons corrected for the penetrability of the incident deuteron, assuming a radius for the $Li^6 + H^2$ system of 1.83 e^2/mc^2. The units are arbitrary and are different for the two curves.
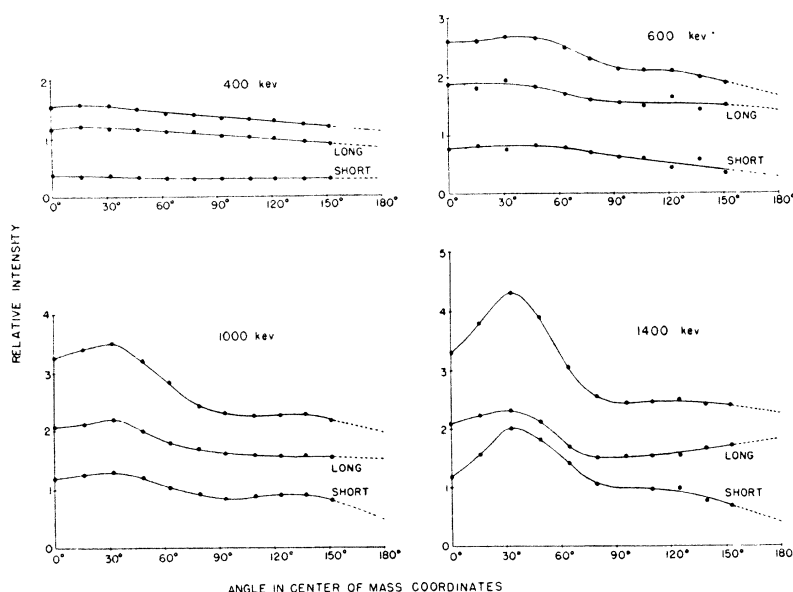
FIG. 4. Angular yield of long and short range proton groups in center of mass coordinates. Proton yield is in arbitrary units but is the same for all curves.

based on the ratio of short to long protons measured with a very thin target mounted on a nickel foil. The cross section indicated in Fig. 2 has been calculated from the weight of the target material as described in the discussion of the alpha-particle excitation curve.

In Fig. 3 are plotted (in arbitrary units) the functions $\sigma^{H^1}(0°)/[P_0(E)\lambda^2]$ obtained by applying the penetrability correction to the experimental excitation functions. The Gamow factor $P_0(E)$ calculated for a nuclear radius of 1.83 e^2/mc^2 for s-deuterons; $\sigma_L^{H^1}$ and $\sigma_S^{H^1}$ are the cross sections for emission of long range and short range protons respectively into unit solid angle at 0°. It should be noted that the two proton groups differ in range by only $4\frac{1}{2}$ cm out of 35 cm (at 1 Mev bombarding energy) and due to straggling the two groups actually overlap, so that range measurements do not provide a complete separation of the two groups. This experimental error is particularly large for the short proton group at low bombarding energy, where the experimental data is the small difference between two larger experimental counting rates. In view of this uncertainty, the fact that the peak in the corrected excitation curve for the long proton group occurs at 400 kev, instead of 374 kev as in the case of the alpha-particles, is not considered significant. The behavior of the short proton group is more ambiguous. Only at the lowest bombarding energy is there an indication of an approach to a peak in the vicinity of 375 kev, and one is reluctant to draw definite conclusions from these data.

IV. PROTON ANGULAR DISTRIBUTION

The angular distribution of the two groups of protons has been observed for bombarding energies of 400, 600, 1000, and 1400 kev. The scattering chamber used in this experiment is a cylindrical brass pill box with aluminum covered observation ports every 15° between 0° and 150°, and a port at 180° to admit the deuteron

beam from the magnetic analyzer. A proportional counter with a window subtending a solid angle of 1.08×10^{-3} steradian can be moved about the perimeter of the cylinder to count protons coming through any of the observation ports. The target, located accurately

TABLE I. Coefficients in the expansion of the proton angular distributions in terms of Legendre polynomials,

$$\sigma(\cos\theta) = \Sigma_i{}^6 A_i P_i(\cos\theta).$$

The units are chosen to make $\sigma(\cos\theta)$ the cross section for emission into unit solid angle.

Bombarding energy		Short proton group	Long proton group	Both groups
		(millibarns)	(millibarns)	(millibarns)
400 kev	A_0	1.14	3.51	4.65
	A_1	<0.01	0.52	0.52
	A_2	0.03	−0.05	−0.01
	A_3	−0.03	0.19	0.16
	A_4	<0.01	−0.14	−0.13
	A_5	−0.03	<0.01	−0.02
	A_6	−0.02	−0.03	−0.05
600 kev	A_0	2.05	5.42	7.46
	A_1	0.83	0.75	1.58
	A_2	−0.25	0.52	0.27
	A_3	<0.01	−0.04	−0.03
	A_4	−0.32	−0.25	−0.57
	A_5	−0.02	−0.19	−0.20
	A_6	<0.01	−0.10	0.10
1000 kev	A_0	2.74	5.67	8.40
	A_1	1.24	1.07	2.31
	A_2	0.59	0.66	1.24
	A_3	0.03	0.08	0.11
	A_4	−0.73	−0.25	−0.99
	A_5	−0.07	−0.23	−0.31
	A_6	0.18	−0.32	−0.14
1400 kev	A_0	3.66	5.45	9.10
	A_1	1.91	0.99	2.92
	A_2	0.58	1.37	1.97
	A_3	−0.06	0.07	0.01
	A_4	−1.21	−0.45	−1.66
	A_5	−0.78	−0.66	−1.44
	A_6	−0.09	−0.45	−0.54

in the center of the chamber, is a thin film of Li₂⁶SO₄ mounted on a thin nickel foil. The thin target, required to give satisfactory resolution of the two proton groups, was not thick enough to stop the deuteron beam at bombarding energies greater than 1500 kev, and our measurements are confined to lower bombarding energies. The target is mounted so that it can be rotated about the axis of the cylinder, perpendicularly to the plane defined by the deuteron beam and the direction of observation.

The following procedure was adopted in determining the angular distributions. At each angle of observation the counting rate was measured with various amounts of aluminum absorber placed in front of the counter window. The counting rate on the plateaus was taken from the integral range-number curve obtained in this way and determines the ratio of long to short protons at the particular angle of observation and bombarding energy used. During these measurements the target was set at the angle which gave the best resolution of the two groups; the consequent variation of target thickness for different angles of observation does not matter, since only the ratio of the two groups is being determined.

The target was next fixed at an angle of 45° with respect to the incident beam, and the total proton counting rate for the two groups together measured over the arc 90° to 150°, counting protons coming from the front surface of the target, and at 0°, counting protons passing through the target backing. The target was then rotated through 90°, so that it presented the same thickness of target material to the incident beam, and the total proton counting rate measured over the arc 0° to 90°, counting protons passing through the target. This procedure was repeated at least twice, taking a count of 2560 protons at each angle. The two sets of data, over the forward and backward angles, were fitted together with the check points at 0° and 90° to give the angular distribution of both groups of protons together. From the ratio of the long group to short group at each angle, the angular distribution of each group alone can be calculated. The observed distribution for both groups and the calculated distribution for each group alone are plotted in Fig. 4 in the center of mass coordinates. Again the correction factor to center of mass coordinates has been calculated for $Q=4.97$ Mev and used for both groups of protons.

In order to gain a quantitative picture of the complexity of these angular distributions the experimental distributions have been expanded in terms of the Legendre polynomials,

$$\sigma(\cos\theta)=\sum_l A_l P_l(\cos\theta)$$
where
$$A_l=\tfrac{1}{2}(2l+1)\int_{-1}^{+1}\sigma(\cos\theta)P_l(\cos\theta)d(\cos\theta).$$

The integration has been carried out numerically by Simpson's method for a second degree polynomial
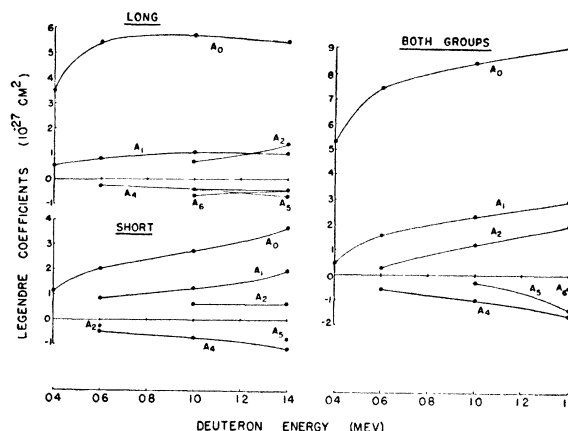

FIG. 5. Coefficients in the expansion of the angular distribution of the proton groups in terms of the Legendre polynomials, plotted as functions of the bombarding energy. The units are chosen so that $\Sigma A_l(E)P_l(\cos\theta)$ is the cross section for proton emission into unit solid angle at the angle Θ. Coefficients not appearing on the graph are less than 0.2×10^{-27} cm².

through the experimental points, taking an interval of $\cos\theta=0.05$ between adjacent points to which the second degree polynomial is fitted. This requires that $\sigma(\cos\theta)$ be known at 41 equally spaced intervals between $\cos\theta=-1$ and $\cos\theta=+1$; these values were taken from the smooth curve drawn through the ten experimental points and extended visually from 150° to 180° as is shown by the dotted sections of the curves in Fig. 4. The values of the coefficients obtained in this way are listed in Table I. The functions defined by these coefficients fit the experimental data to within less than the experimental error; for example, the deviation between the experimental distribution for the two groups together at 1.4 Mev, the case of greatest complexity, and the function defined by the calculated coefficients is less than 3 percent. In Fig. 5 these coefficients have been plotted as functions of the bombarding energy. Note that $4\pi A_0$ is the total integrated cross section. For the two groups together, where the experimental accuracy is best, the coefficients show a uniform variation with energy. For the individual proton groups the same general behavior is apparent, with some slight differences that probably indicate the limits of accuracy of these measurements.

Theoretical interpretation of these angular distributions is beyond the scope of this paper. However, it may be noted that the appearance of terms as high as P_4 and P_6 in the expansion may be interpreted to indicate that d and f deuterons take part in the reaction leading to the emission of protons at these bombarding energies. Inglis has already found evidence for the excitation of levels in Be⁸ by d-deuterons in this energy range from the angular distribution of the alpha-particles in the Li$(d,\alpha)\alpha$ reaction; f-deuterons do not take part in the alpha-particle reaction.[3]

One of the authors (W.W.) was aided during the course of this work by an AEC fellowship.